[CANCER RESEARCH 63, 6825–6837, October 15, 2003]

Induction of Apoptosis by the Garlic-Derived Compound *S*-Allylmercaptocysteine (SAMC) Is Associated with Microtubule Depolymerization and c-Jun NH_2-Terminal Kinase 1 Activation[1]

Danhua Xiao, John T. Pinto, Jae-Won Soh, Atsuko Deguchi, Gregg G. Gundersen, Alexander F. Palazzo, Jung-Taek Yoon, Haim Shirin, and I. Bernard Weinstein[2]

Institute of Human Nutrition [D. X.], Herbert Irving Comprehensive Cancer Center [J-W. S., A. D., J-T. Y., I. B. W.], Department of Anatomy and Cell Biology [G. G. G., A. F. P.], College of Physicians and Surgeons, Columbia University, New York, New York 10032; American Health Foundation, Valhalla, New York 10595 [J. T. P.]; and E. Wolfson Medical Center, Holon, 58100 Israel [H. S.]

ABSTRACT

Epidemiological and experimental carcinogenesis studies provide evidence that components of garlic (*Allium sativum*) have anticancer activity. We recently reported that the garlic derivative *S*-allylmercaptocysteine (SAMC) inhibits growth, arrests cells in G_2-M, and induces apoptosis in human colon cancer cells (Shirin *et al.*, Cancer Res., *61:* 725–731, 2001). Because a fraction of the SAMC-treated cells are specifically arrested in mitosis, we examined the mechanism of this effect in the present study. Immunofluorescent microscopy revealed that the treatment of SW480 cells or NIH3T3 fibroblasts with 150 μM SAMC (the IC_{50} concentration) caused rapid microtubule (MT) depolymerization, MT cytoskeleton disruption, centrosome fragmentation and Golgi dispersion in interphase cells. It also induced the formation of monopolar and multipolar spindles in mitotic cells. *In vitro* turbidity assays indicated that SAMC acted directly on tubulin to cause MT depolymerization, apparently because it interacts with −SH groups on tubulin. To investigate the signaling pathways involved in SAMC-induced apoptosis, we assayed c-Jun NH_2-terminal kinase (JNK) activity and found that treatment with SAMC caused a rapid and sustained induction of JNK activity. The selective JNK inhibitor SP600125 inhibited the early phase (24 h) but not the late phase (48 h and later) of apoptosis induced by SAMC. Expression of a dominant-negative mutant of JNK1 in SW480 cells inhibited apoptosis induced by SAMC at 24 h but had no protective effect at 48 h. $JNK1^{-/-}$ mouse embryonic fibroblasts were resistant to SAMC-induced apoptosis at 24 h but not at 48 h. On the other hand, the inhibition or abrogation of JNK1 activity did not inhibit the G_2-M arrest induced by SAMC. SAMC also activated caspase-3. The general caspase inhibitor z-VAD-fmk inhibited both early and late phases of apoptosis induced by SAMC. We conclude that the garlic-derived compound SAMC exerts antiproliferative effects by binding directly to tubulin and disrupting the MT assembly, thus arresting cells in mitosis and triggering JNK1 and caspase-3 signaling pathways that lead to apoptosis.

INTRODUCTION

Garlic, a plant within the genus *Allium*, has been used for disease prevention and treatment in many different cultures, especially for diseases of the gastrointestinal tract. Epidemiological investigations in China, Italy, and America have provided evidence that the risks of stomach and colon cancers are inversely related to regular consumption of garlic and garlic products (1). Experimental carcinogenesis studies indicate that components of garlic (*e.g.*, allyl sulfides) inhibit both the initiation and promotion stages of tumorigenesis for various types of cancer, including colorectal, lung, and skin cancers (1). We recently reported that the naturally occurring water-soluble garlic derivative SAMC,[3] but not SAC, inhibits growth, arrests cell cycle progression at the M phase, and induces apoptosis in SW480 and HT 29 human colon cancer cells (2).

MTs are major cellular structural components. They play important roles in the development and maintenance of cell shape, cell replication and division, cell signaling, and cellular movement. MTs are composed of a backbone of α- and β-tubulin heterodimers and smaller amounts of MAPs. They are in an unstable steady state of a highly dynamic process of polymerization and depolymerization, which can be influenced by numerous factors (3). Certain cancer chemotherapy agents exert their antitumor actions by disrupting the dynamics of MT assembly, thus perturbing the formation and function of the mitotic spindle apparatus and arresting cells in mitosis. These agents are called MIAs. For example, paclitaxel (Taxol) binds to and stabilizes MTs, whereas Colcemid and *Vinca* alkaloids bind to and depolymerize MTs (4). An in-depth understanding of the molecular mechanisms by which these and other MIAs act may enhance their use in both cancer prevention and chemotherapy.

Because we found that a fraction of the SAMC-treated cells are specifically arrested in mitosis, in the present study we examined the effects of this compound on MTs. We found that SAMC can act directly to cause MT depolymerization and thereby disrupt the MT cytoskeletal network in interphase cells and also interfere with spindle formation in mitotic cells. We also obtained evidence that the activation of JNK1 and caspase-3 play important roles in SAMC-induced apoptosis. These novel effects of SAMC provide new insights into the molecular mechanisms responsible for the antitumor effects of this compound and may encourage further application of this and related compounds to cancer treatment and prevention.

MATERIALS AND METHODS

Allium Derivatives. SAMC and SAC are water-soluble allium derivatives and were generously supplied by Wakunaga of America Co., Ltd. (Mission Viejo, CA). Stock solutions of SAMC and SAC (10 mM) were prepared fresh in PBS.

Chemicals and Antibodies. The selective JNK1 inhibitor SP, p38 inhibitor SB, MEK1/2 inhibitor PD, and general caspase inhibitor VAD were purchased from Calbiochem (La Jolla, CA). The fluorogenic tetrapeptide substrates of caspase-1 (Z-YVAD-AFC), caspase-6 (Ac-VEID-AMC), and caspase-9 (Ac-LEHD-AFC) were purchased from Calbiochem. The fluorogenic substrates of caspase-3 (Ac-DEVD-AFC) and caspase-8 (Ac-IETD-AFC) were purchased

Received 2/13/03; revised 7/16/03; accepted 7/22/03.

The costs of publication of this article were defrayed in part by the payment of page charges. This article must therefore be hereby marked *advertisement* in accordance with 18 U.S.C. Section 1734 solely to indicate this fact.

[1] Supported by funding from the National Foundation for Cancer Research and the T. J. Martell Foundation (to I. B. W.), the NIH Grant GM62939 (to G. G. G.), and the NIH Grant CA89815 (to J. T. P.).

[2] To whom requests for reprints should be addressed, at the Herbert Irving Comprehensive Cancer Center, College of Physicians and Surgeons, Columbia University, Columbia-Presbyterian Medical Center, 701 West 168th Street, Suite 1509, New York, NY 10032. Phone: (212) 305-6921; Fax: (212) 305-6889; E-mail: ibw1@columbia.edu.

[3] The abbreviations used are: SAMC, *S*-allylmercaptocysteine; dn, dominant negative; EGFP, enhanced green fluorescent protein; ERK, extracellular signal-regulated kinase; JNK, c-Jun NH_2-terminal kinase; MAPK, mitogen-activated protein kinase; MEF, mouse embryonic fibroblast; MT, microtubule; MAP, MT-associated protein; MIA, MT-interfering agent; SAC, *S*-allylcysteine; β-ME or BME, β-mercaptoethanol; TPA, 12-*O*-tetradecanoylphorbol-13-acetate; WT, wild type; SB, SB203580; SP, SP600125; PD, PD98059; VAD, z-VAD-fmk; PI, propidium iodide; CMV, cytomegalovirus; TBS, Tris-buffered saline; DMBA, 7,12-dimethylbenz(a)anthracene; 7-AAD, 7-amino-actinomycin; AFC, 7-amino-4-trifluoromethylcoumarin; AMC, 7-amino-4-methylcoumarin; G-PEM, buffer composed of GTP, PIPES, EGTA and $MgCl_2$.

from PharMingen (San Diego, CA). Primary antibodies used in Western blotting for ERK1/2, phospho-ERK1/2, p38, and phospho-p38 were obtained from Cell Signaling Technology (Beverly, MA), and the antibody to actin was obtained from Sigma-Aldrich Biotechnology (St. Louis, MO). Paclitaxel (Taxol) and cytochalasin D were obtained from Sigma, and Colcemid (*N*-methyl-*N*-deacetyl-colchicine) was obtained from Roche (Indianapolis, IN).

Cell Lines and Culture Conditions. The human colon cancer SW480 and mouse fibroblast NIH3T3 cell lines were obtained from the American Type Culture Collection (Manassas, VA). The cultures of WT MEF cells ($JNK^{+/+}$), MEF $JNK1^{-/-}$ cells, and MEF $JNK2^{-/-}$ cells were established from mutant mice with the respective genotypes (5) and were generously provided by Dr. Zigang Dong (University of Minnesota, Austin, MN). SW480 cells and MEF cells were grown in DMEM with 10% fetal bovine serum, and NIH3T3 cells were grown in DMEM with 10% calf serum (Life Technologies, Inc., Grand Island, NY). Cells were incubated in a 100% humidified incubator at 37°C with 5% CO_2. All of the biochemical studies were performed with exponentially growing cells at 50% confluence.

Cell Cycle Analysis. PI staining was used to analyze DNA content, as reported previously (6). After the desired time of exposure to the indicated compounds, both adherent and floating cells were harvested, fixed with 70% ethanol, incubated with PI (0.05 mg/ml) and 1 μg/ml RNase A (Sigma) at room temperature in the dark for 30 min, and analyzed by flow cytometry, using a FACS Calibur instrument with a CellQuest software (Becton Dickinson, San Jose, CA). The apoptotic cells were considered to constitute the sub-G_1 population, and the percentage of nonapoptotic cells in each phase of cell cycle was determined. All of the experiments were performed at least twice and yielded similar results.

Apoptosis Assay. The percentage of cells undergoing apoptosis was determined by Annexin V-PE assay, as described previously (6). Briefly, after the cells were treated with either PBS (control) or SAMC (300 μM) for the desired time, both adherent and floating cells were harvested and double stained with Annexin V-PE (stained apoptotic cells) and 7-AAD (stained dead cells; PharMingen). The percentage of apoptotic cells was then determined by flow cytometric analysis. All of the experiments were performed three times, independently, and the results are expressed as mean ± SD.

Transfection and Flow Cytometric Analyses. SW480 cells were transfected with either the control vector pcDNA3 or pcDNA3-DN-JNK1, by a liposome-mediated method using the Lipofectin Reagent (Invitrogen Life Technologies, Inc., Carlsbad, CA). The pcDNA3-DN-JNK1 plasmid encodes a FLAG epitope-tagged, kinase-inactive dn JNK1 and was generated from a pCMV-DN-JNK1 plasmid by subcloning and neomycin selection (7). The pCMV-DN-JNK1 was kindly provided by Dr. Audrey Minden (Ref. 8; Columbia University, New York, NY). A CMV promoter-driven farnesylated-EGFP construct, pEGFPF, was cotransfected as a selectable marker for transfected cells (9). The pEGFPF plasmid was kindly provided by Dr. Wei Jiang (The Salk Institute, La Jolla, CA). After a 24-h transfection, the cells were

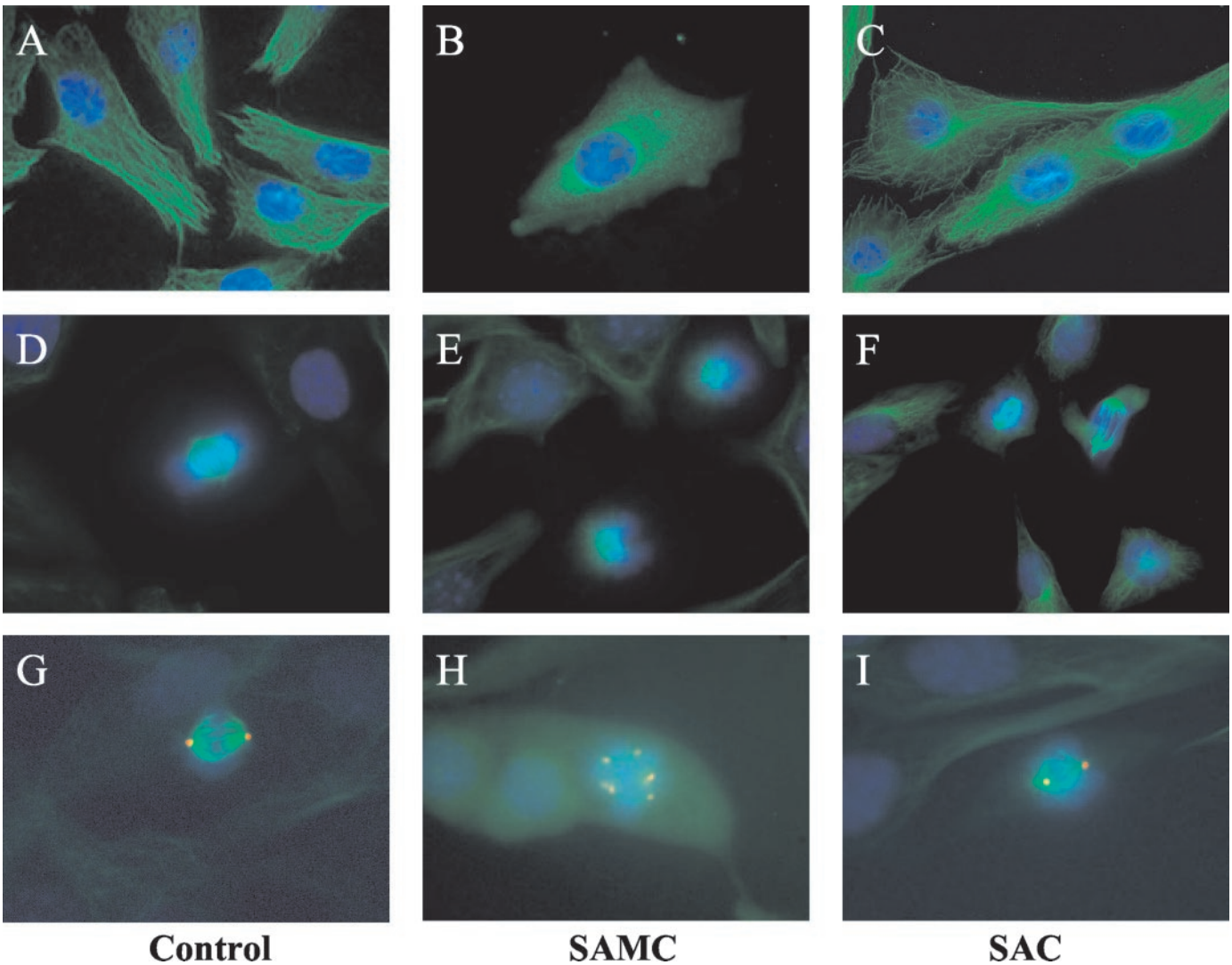

Fig. 1. Immunofluorescence microscopy. NIH3T3 cells were treated with PBS (control), 150 μM SAMC or SAC for 24 h, fixed with methanol, and immunostained for MT (*green*), centrosome (*red*), and DNA (*blue*), with the respective antibodies, and then were visualized by indirect immunofluorescence, as described in "Materials and Methods." *A, D, G,* control cells; *B, E, H,* SAMC-treated cells; *C, F, I,* SAC-treated cells; *A–C,* interphase cells; *D–I,* mitotic cells. MTs are depolymerized and MT networks are disrupted in the SAMC-treated interphase cells. The spindle apparatus are abnormal (monopolar or multipolar) in the SAMC-treated mitotic cells. (*A, B, C, E, F, H,* ×600; *D, G, I,* ×1000.)

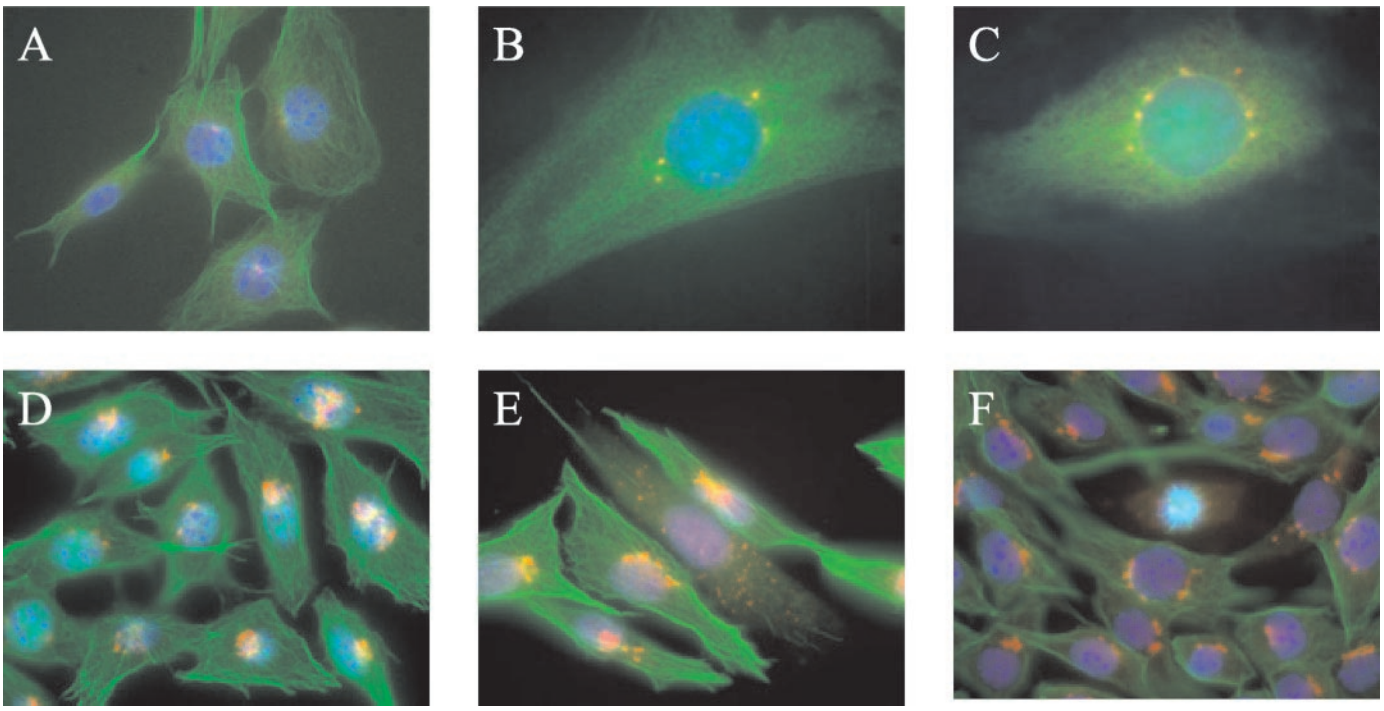

Fig. 2. Immunofluorescence microscopy. NIH3T3 cells were treated with PBS (control) or SAMC for different time periods, fixed with methanol, and immunostained for MT (*green*), DNA (*blue*), centrosome (*red*, *A–C*), or Golgi (*red*, D–F), with the respective antibodies, and then were visualized by indirect immunofluorescence, as described in "Materials and Methods." *A*, *D*, control; *B*, *C*, SAMC (150 μM), 10 min and 1 h, respectively; *E*, SAMC (150 μM), 24 h, interphase cells; *F*, SAMC (150 μM), 24 h, a mitotic cell in the center. SAMC (150 μM) induced MT depolymerization and centrosome fragmentation as early as 10 min. It also caused dispersed distribution of Golgi stacks in both interphase and mitotic cells. (×600.)

treated with either PBS (control) or SAMC (300 μM) for the indicated times (18, 24 or 48 h). Both adherent and floating cells were harvested, double stained with Annexin V-PE and 7-AAD, and analyzed by flow cytometry. The early apoptotic transfected cells were determined as the 7-AAD-negative, GFP-positive and Annexin V-PE-positive cells, and the percentage in live transfected cells (7-AAD-negative, GFP-positive cells) was calculated. Aliquots of the cells were also stained with PI after treatment with SAMC, and the cell cycle distribution among transfected cells was analyzed by DNA flow cytometry.

Protein Extraction and Western Blotting. The methods for protein extraction and Western blot analysis have been described previously (6). Briefly, after treatment with the indicated compounds for the desired time, both adherent and floating cells were collected and cell lysates were prepared. Protein concentrations were determined using the Bio-Rad Protein assay (Bio-Rad, Richmond, CA). Protein samples, 50 μg each, were subjected to SDS-PAGE, transferred to nitrocellulose membranes (Millipore, Bedford, MA), and blocked with 5% milk protein. Membranes were then incubated with the indicated primary antibody for 1 h or overnight, depending on the antibody, and were incubated with the corresponding horseradish peroxidase-conjugated secondary antibody for 1 h. Protein-antibody complexes were detected by an enhanced chemiluminescence system (Amersham, Piscataway, NJ). Immunoblotting for actin was performed to verify equivalent amounts of loaded protein. Results were analyzed on a Macintosh computer using the public domain NIH Image program (developed at the United States NIH and available on the Internet at http://rsb.info.nih.gov/nih-image/).

Indirect Immunofluorescence Microscopy. The immunostaining method was essentially as described by Yoon *et al.* (10), with some modifications. Briefly, cells were grown on glass coverslips in 6-well plates (35-mm diameter). After exposure to PBS (control), 150 μM SAMC, or SAC for the indicated time period, the cells were washed once in DMEM at 37°C and were fixed with methanol at −20°C for 10 min. Fixed cells were washed three times with TBS for 10 min and were incubated with TBS, 10% normal goat serum, (Vector Labs, Burlingame, CA) plus the proper concentration of the primary antibody, as described below, for 1 h at 37°C in a 100% humidified chamber. After three washes with TBS, the cells were incubated with TBS and 10% normal goat serum plus the appropriate secondary antibody, as described below, for 45 min at 37°C in a 100% humidified chamber. After incubation, the cells were washed three times with TBS and refixed with 4% formaldehyde for 10 min. Coverslips were rinsed with tap water, mounted with Histomount (Vector Labs), and sealed to the microscope slide with clear nail polish. The slides were observed with a Nikon Optiphot microscope, and images were captured with a MicroMax cooled CCD (charge-coupled device) camera (Kodak KAF 1400 chip; Princeton Scientific Instruments, Monmouth Junction, NJ) using Metamorph software (Universal Imaging, Downingtown, PA).

Cells were stained for MTs with a rat monoclonal antibody against tyrosinated α-tubulin (YL1/2; 1:10 dilution; Ref. 11) and visualized with a goat antirat IgG-FITC conjugate (1:100; Chemicon International Inc., Temecula, CA). Cells were stained for centrosomes with a rabbit antipericentrin antibody (1:200; Babco, Richmond, CA) or Golgi complex with a rabbit anti-Giatin antibody (1:200) and were visualized with a goat antirabbit IgG-rhodamine conjugate (1:200), and were also stained with 4′,6-diamidino-2-phenylindole (DAPI; 1:1000) to visualize DNA.

Tubulin Turbidity Assay. *In vitro* MT and tubulin assembly were monitored by the turbidity assay. Fifty μl of 5 mg/ml pure tubulin (Cytoskeleton, Denver, CO) was assembled to a steady state in G-PEM buffer [100 mM PIPES (pH 6.9), 1 mM EGTA, 1 mM $MgCl_2$, and 1 mM GTP] plus 10% glycerol in 96-well plate (0.33 cm^2/well), by incubation at 37°C for 20–30 min. This is referred to as the "polymer stock." The tested compounds were prepared in G-PEM buffer at 3.5 times the indicated final concentrations and prewarmed to 37°C. Twenty μl of the test-compound solution was pipetted into the polymer stock wells and the plate was incubated at 37°C for an additional 20–30 min. The effects on polymerization/depolymerization of the tested compounds were quantitated by measuring the increase/decrease of the absorbance at 340 nm (A_{340}) over time, using a Spectramax O.D. Reader and SOFTmax PRO 3.0 software (Molecular Devices, Sunnyvale, CA) in a kinetic model (one reading/min). Similar assays were also performed with MAP-rich tubulin (Cytoskeleton) instead of pure tubulin at 1 mg/ml in G-PEM buffer, without glycerol. In all of the assays the absorbance at 340 nm of the tested compound itself was subtracted from the total absorbance. Results are presented as a percentage of absorbance, with 100% representing the A_{340} value at 20 or 30 min, when the tubulin polymerization reached a steady state.

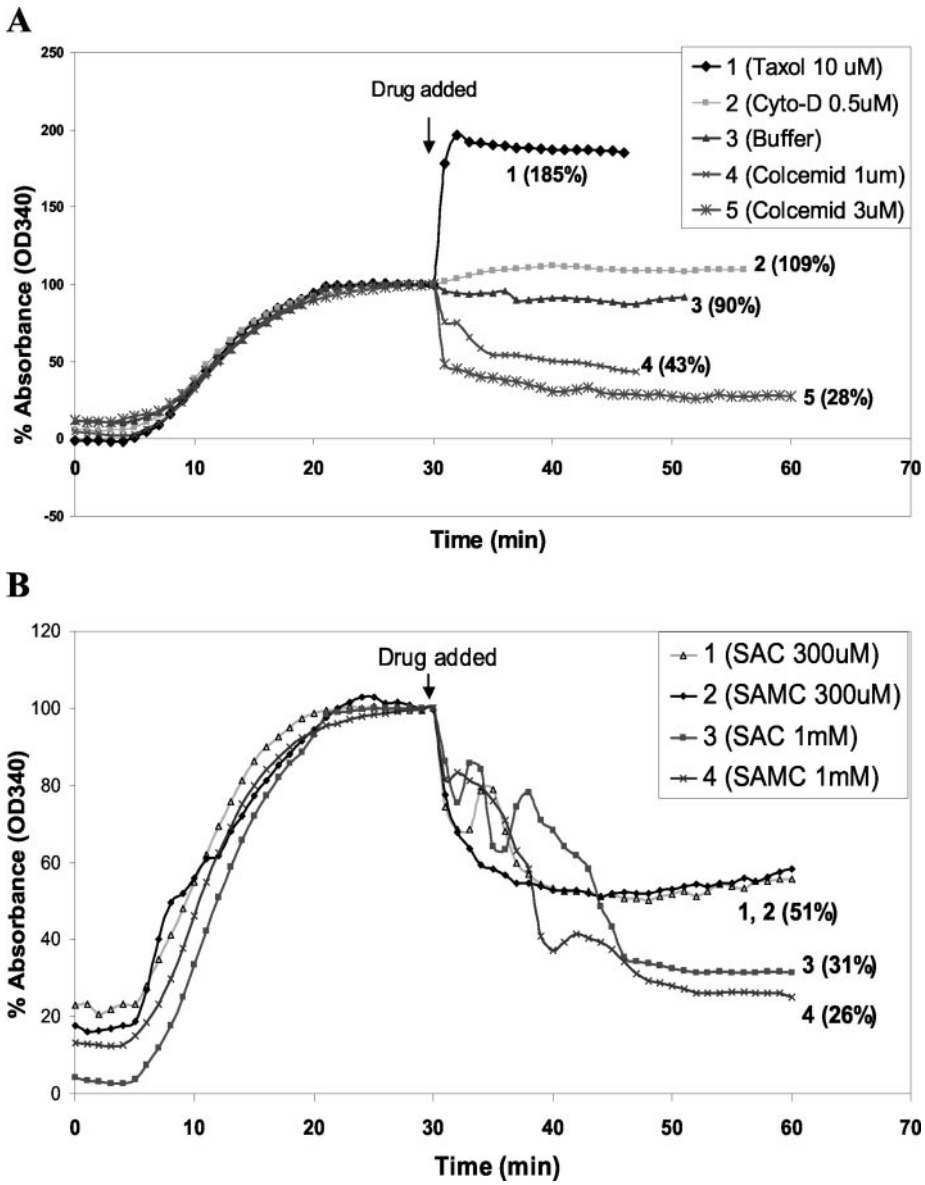

Fig. 3. Effects of SAMC and SAC on *in vitro* MT polymerization. Pure tubulin (5 mg/ml; *A*, *B*, and *D*) or MAP-rich tubulin (1 mg/ml; *C*) was incubated at 37°C for 20–30 min, and then the indicated compounds were added at the indicated concentrations. A_{340} values were recorded once per min for an additional 20–30 min. The results are presented as percentage of absorbance, with 100% representing the A_{340} value at 20 or 30 min when the tubulin polymerization had reached a steady state, after which the compounds were added. The data in parentheses indicate the final percentage of absorbance after each compound was added. *Cyto-D*, cytochalacin D.

JNK Activity Assay. A nonradioactive kinase assay was used according to the instruction manual of Cell Signaling Technology, Inc. Briefly, after the cells were treated with PBS (negative control) or SAMC at the indicated concentrations and times, the media were removed, and the cells were rinsed once with ice-cold PBS and scraped off the plate. Cells were also exposed to a germicidal UV lamp (254 nm, 30 W, 70-cm distance between plates and the UV lamp) in a cell culture hood for 30 min as a positive control for activating JNK. The UV dose was ~40 J/m^2 (12). Cell pellets were then suspended in 500 μl of M2 lysis buffer [20 mM Tris (pH 7.6) containing 0.5% NP40, 250 mM NaCl, 3 mM EDTA, 3 mM EGTA, 1 mM DTT, 1 μg/ml leupeptin, 0.02 M β-glycerophosphate, 1 mM sodium orthovanadate and 1 mM phenylmethylsulfonyl fluoride]. JNK1 was immunoprecipitated by incubation of 200 μg of this cell protein extract with 2 μg (20 μl) of c-Jun fusion protein beads (Cell Signaling), with gentle rocking overnight at 4°C. The precipitates were washed twice with M2 buffer and twice with kinase buffer [25 mM Tris (pH 7.5) containing 10 mM $MgCl_2$, 5 mM β-glycerophosphate, 2 mM DTT, and 0.1 mM Na_3VO_4]. Pellets were suspended in 50 μl of kinase buffer supplemented with 100 μM ATP and were incubated at 30°C for 30 min. The kinase reaction was terminated by adding 25 μl of 3× SDS sample buffer, and the reaction mixtures were boiled for 5 min. Samples were analyzed by Western blotting using a phospho-c-Jun (Ser63) antibody (1:1000 dilution; Cell Signaling).

Caspase Activity Assay. After treatment with SAMC or SAC (300 μM) for the indicated times, the cells were washed twice with ice-cold PBS and harvested and extracts prepared as described previously (2). Caspase activity was determined using a fluorometric assay. Briefly, 10 μg of total protein were incubated with 2 μg of the fluorogenic peptide substrates Z-YVAD-AFC, Ac-DEVD-AFC, Ac-VEID-AMC, Ac-IETD-AFC, or Ac-LEHD-AFC, the fluorogenic substrate for caspase 1, -3, -6, -8-, or -9, respectively, in a 200-μl caspase buffer at 37°C for 3 h. The release of AFC or AMC was measured with a Gemini Fluoro/Luminometer (Molecular Devices) at an excitation wavelength of 400 or 360 nm and an emission wavelength of 505 or 460 nm, respectively. Results are presented as the fold increase of caspase activity, as compared with that of the untreated control cells.

Statistical Analysis. Data are expressed as mean ± SD. Comparisons between control cells and drug-treated cells were made using Student's *t* test. A difference between groups with $P < 0.05$ were considered statistically significant.

RESULTS

SAMC Depolymerizes MTs, Induces Centrosome and Golgi Fragmentation in Interphase Cells, and Interferes with the Spindle Assembly in Mitotic Cells. In view of our previous studies indicating that SAMC inhibits growth and arrests SW480 cells in mitosis (2), we examined the possible effects of this compound on the cellular MT system and on spindle assembly, because MTs are major

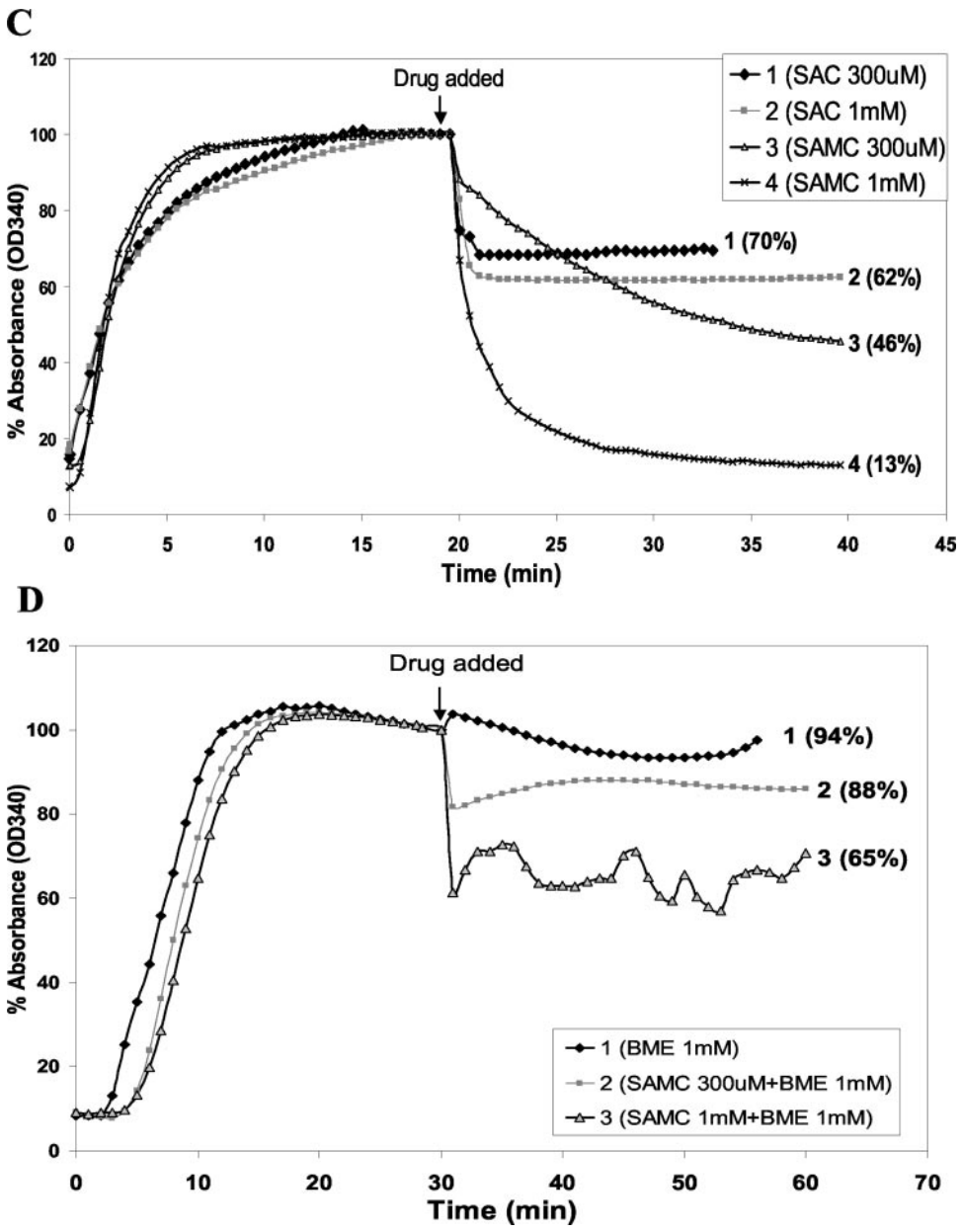

Fig. 3. *Continued.*

structural components of the cytoskeleton and mitotic spindles and play essential roles in the process of mitosis. We examined the effects of SAMC on SW480 human colon cancer cells as well as on NIH3T3 mouse fibroblast cells, because the latter cell line is a well-characterized model system for examining MTs (13). Immunostaining with the rat-YL1/2 anti-tyrosinated α-tubulin antibody and a goat antirat IgG-FITC conjugate indicated that treatment of NIH3T3 cells with 150 μM SAMC (the IC_{50} concentration for growth inhibition) for 24 h caused extensive MT depolymerization and disruption of the MT network in interphase cells (Fig. 1*B*). In addition, treatment with SAMC interfered with the normal spindle formation in M-phase cells. There was a marked increase of mitotic cells with monopolar spindles, which contained a ring of condensed chromosomes and a monopolar spindle pole in the center with astral MTs irradiating from it (Figs. 1*E* and 2*F*). Multipolar spindles were also observed in some of the SAMC-treated mitotic cells, together with abnormal chromosome alignments (Fig. 1*H*). Bipolar spindles, which were present in control cells (Fig. 1, *D* and *G*), were hardly seen in SAMC-treated cells. As expected from our previous studies (2), SAC (150 μM) did not show any effect on MTs or mitotic spindles in these cells (Fig. 1, *C*, *F*, and *I*). A time course study indicated that the depolymerization effect of SAMC on MTs occurred as early as 10 min after treatment (Fig. 2*B*). Using antibodies to pericentrin or Giatin, we observed additional effects of SAMC on cells. Treatment of interphase cells with SAMC caused fragmentation of the centrosome (Fig. 2, *B* and *C*). It also disrupted the distribution of the Golgi complex (Fig. 2*E*), when compared with the control cells in which the Golgi stacks were gathered juxtanuclearly (Fig. 2*D*). As expected (14), the Golgi elements were dispersed throughout the cytoplasm in untreated mitotic cells, and this was also seen in SAMC-treated mitotic cells (Fig. 2*F*). Studies with SW480 cells indicated that SAMC produced effects on MT depolymerization in interphase cells and abnormal spindle formation in mitotic cells, similar to those described above with NIH3T3 cells (data not shown).

SAMC Causes Direct *in Vitro* Depolymerization of MTs. To determine whether SAMC has a direct effect on tubulin polymerization/depolymerization, we performed *in vitro* tubulin turbidity assays. Pure tubulin (5 mg/ml in G-PEM buffer) was incubated at 37°C for 30

min. When the turbidity (A_{340}) indicated that tubulin polymerization had reached a plateau, the test compounds were added. As expected (15, 16), the addition of Taxol caused increased tubulin polymerization, the addition of Colcemid caused decreased tubulin polymerization, and the addition of cytochalasin D (a well-known anti-actin, but not anti-tubulin, compound) or simply the G-PEM buffer had no significant effect (Fig. 3*A*). The addition of 300 μM SAMC caused about a 50% decrease in tubulin polymerization (Fig. 3*B, curve 2*), and an even greater effect was seen with 1 mM SAMC (Fig. 3*B, curve 4*). We were surprised to find that in these *in vitro* assays with pure tubulin, SAC had an effect on MT depolymerization similar to that obtained with SAMC (Fig. 3*B, curves 1* and *3*), although in living cells, SAC did not inhibit cell proliferation (2) and had no detectable effect on MT depolymerization (Fig. 1). Because of this apparent discrepancy, we conducted *in vitro* turbidity assays with MAP-rich tubulin, to more closely resemble the situation in intact cells. In this system, SAC still induced MT depolymerization (Fig. 3*C, curves 1* and *2*), but the effect was much weaker than that obtained with an equivalent concentration of SAMC (Fig. 3*C, curve 3* and *4*). These findings suggest that the MAPs partially protect MT from the depolymerizing effect of SAC, although other factors probably also play a role in explaining why SAC lacks cytotoxicity in cultured cells (see "Discussion").

SAMC May Interact with the Sulfhydryl Groups on Tubulin. It is known that tubulin contains distinct binding sites for colchicine and for vinblastine (17). Competitive binding assays with fluorescent colchicine and vinblastine indicated that SAMC in doses up to 1 mM did not inhibit the binding of colchicine or vinblastine to tubulin (data not shown), suggesting that SAMC binds to a site on tubulin that is different from the site on colchicine and vinblastine. Because SAMC is an organosulfur compound, it is possible that it may form disulfide bonds with thiol-containing amino acids in tubulin. Therefore, we used β-ME, a known reducing agent with one $-$SH/molecule, which has been used to inhibit disulfide formation in other proteins (18). As shown in Fig. 3*D*, β-ME (1 mM) itself had no significant effect on tubulin polymerization (*curve 1*). SAMC still caused a decrease in tubulin polymerization in the presence of 1 mM β-ME, but this effect was markedly reduced. Tubulin polymerization was decreased by 49% after the addition of 300 μM SAMC alone (Fig. 3*B, curve 2*), but was decreased by only 12% after the addition of 300 μM SAMC and 1 mM β-ME (Fig. 3*D, curve 2*). One mM SAMC decreased tubulin polymerization by 74% (Fig. 3*B, curve 4*), whereas it decreased tubulin polymerization by only 35% when added together with 1 mM β-ME (Fig. 3*D, curve 3*). These data suggest that there is competitive binding between SAMC and β-ME to thiol ($-$SH) groups in tubulin, and provide evidence that thiol groups of amino acids in tubulin (*i.e.,* cysteine residues) may be the binding sites for SAMC (see "Discussion").

SAMC Induces JNK1 Activation. Activation of JNK1 plays an important role in mediating the apoptosis induced by various toxic agents, including the MT-stabilizing agent Taxol and the MT-depolymerizing agent vinblastine (12). To investigate the signaling pathways involved in SAMC-induced apoptosis, we measured stress-activated protein kinase (SAPK)/JNK activity in extracts of SAMC-treated SW480 cells using a nonradioactive *in vitro* kinase assay. The cells were also treated with 40 J/m^2 UV as a positive control (Fig. 4). Treatment of cells with 300 μM SAMC induced a rapid (within 15 min after treatment) and strong (3.5-fold increase) activation of JNK, which persisted for up to 12 h, with fluctuations in intensity during this interval including a decrease at 6 h (Fig. 4*A*). Additional studies, including the transient decrease at 4–6 h (data not shown), confirmed these results.

The Selective JNK Inhibitor SP Inhibits the JNK1 Activation and Early-Phase Apoptosis, but not Late-Phase Apoptosis or G_2-M Cell Cycle Arrest Induced by SAMC. To further investigate the role of JNK1 in SAMC-induced cellular events, we used a novel JNK inhibitor SP, which has been shown to have a 300-fold selectivity for JNK in *in vitro* kinase assay (IC_{50} 40–100 nM) and at least a 10-fold selectivity for the JNK pathway in cultured cells, when assayed for inhibition of c-Jun phosphorylation at 10–50 μM (19, 20). Because of the nonspecific cytotoxicity of SP when cells were treated with the drug for more than 6 h (data not shown), we pretreated SW480 cells with 0, 20, 50, or 100 μM SP for 4 h, removed this medium, and then treated the cells with SAMC (300 μM) for 15 min–48 h. SP itself had no effect on JNK1 activity. Pretreatment of SW480 cells with 50 μM SP partially inhibited, and pretreatment with 100 μM SP markedly inhibited, SAMC-induced JNK1 activation (Fig. 4*B*). We found that pretreatment of cells with 100 μM SP also caused about a 50% inhibition of SAMC (300 μM)-induced apoptosis when assayed at 24 h after the addition of SAMC (Fig. 5, *A* and *B*). It is of interest that this effect was highly time dependent because pretreatment with 100 μM SP caused only 20% inhibition at 48 h, and no inhibition of apoptosis occurred at 72 h (Fig. 5*B*). By contrast, during this time course within the nonapoptotic population, pretreatment of cells with 100 μM SP did not inhibit the G_2-M arrest induced by SAMC and, in fact, enhanced it (Fig. 5*C*). The fact that SP did not inhibit the accumulation of SAMC-treated cells in G_2-M is consistent with our evidence that SAMC induces cells to arrest in M phase by directly binding to tubulin and causing MT depolymerization (Fig. 3). Therefore, the latter effects are independent of JNK1 activation.

Expression of dn-JNK1 Inhibits Apoptosis Induced by SAMC at 18 and 24 h, but not at 48 h. To confirm the above effects of the JNK inhibitor SP on SAMC-induced apoptosis, we did similar studies using a dn mutant of JNK1. SW480 cells were transfected with a dn-JNK1 or a control vector plasmid, along with fluorescent marker pEGFPF to allow selection for the transfected cells. After 24 h of transfection, the cells were treated with 300 μM SAMC for the indicated times, stained with Annexin V-PE and 7-AAD, and analyzed by flow cytometry; the percentage of early apoptotic cells within the transfected population was then calculated. As shown in Fig. 6*A*, expression of dn-JNK1 in these cells inhibited SAMC-induced apoptosis, and this inhibition was highly time-dependent. At 18 h, SAMC treatment caused about a 2-fold increase in apoptosis in the vector-transfected cells, and at this early time point, the apoptosis induced by SAMC was almost completely abolished by the expression of dn-JNK1. However, at the 24 and 48 h time points, the expression of dn-JNK1 inhibited SAMC-induced apoptosis by only 50 and 25%, respectively. These results are consistent with the data obtained in Fig. 5*B* with the SP JNK inhibitor, thus providing further evidence that JNK1 plays a more important role in mediating the early phase than the late phase of apoptosis induced by SAMC. The dn-JNK1-transfected cells were also stained with PI and analyzed by flow cytometry for cell cycle distribution. Expression of dn-JNK1 did not inhibit the G_2-M arrest induced by SAMC (data not shown).

JNK1$^{-/-}$ MEF Cells Are Resistant to SAMC-Induced Apoptosis at 18 and 24 h, but not at 48 h. To further study the role of JNK1 and to also examine the possible role of JNK2 in SAMC-induced apoptosis, we used cultures of WT MEF cells (JNK$^{+/+}$), MEF JNK1$^{-/-}$ cells, and MEF JNK2$^{-/-}$ cells that were established from mutant mice with the respective genotypes (5). The three types of cells were treated with 300 μM SAMC for 18, 24, or 48 h, and then were stained with Annexin V-PE and 7-AAD, or with PI, and were analyzed by flow cytometry. As shown in Fig. 6*B*, at both the 18 and 24 h time points, the extent of apoptosis induced by SAMC in the JNK1$^{-/-}$ cells was significantly less than that in the WT MEF cells.

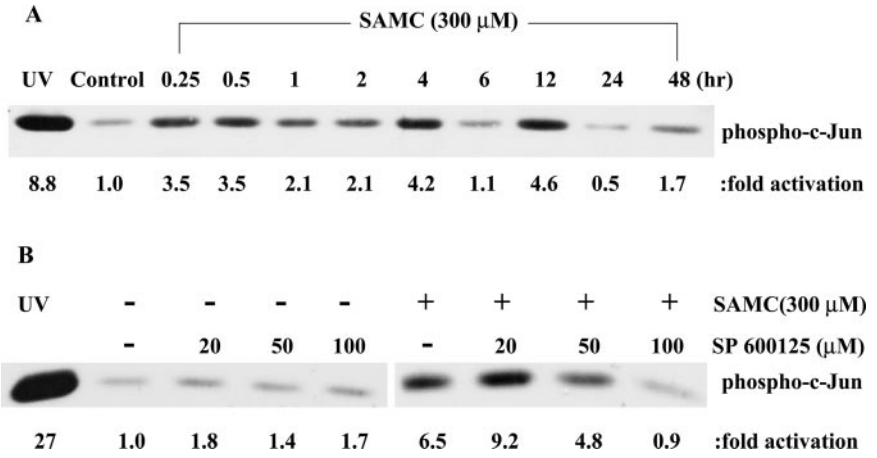

Fig. 4. Effects of SAMC on activation of JNK1 kinase. *A*, SAMC induces JNK1 activation in SW480 cells. Cells were treated with SAMC (300 μM) for the indicated times, and JNK kinase assays were performed as described in "Materials and Methods." *B*, SP inhibits SAMC-induced JNK1 activation in a dose-dependent manner. Cells were pretreated with the indicated concentrations of SP for 4 h; then the medium was removed, the cells were treated with SAMC (300 μM) for another 12 h, and the JNK kinase assays were performed. Cells were also treated with 40 J/m^2 UV as a positive control, and assayed at 30 min. Data shown are from a representative experiment. "Fold activation" is expressed relative to the control value obtained with untreated cells. Similar results were obtained in two additional studies.

However, there was no significant difference between these two cell lines with respect to the extent of apoptosis induced at 48 h. Thus, a lack of JNK1 activity makes these cells relatively resistant to SAMC-induced apoptosis at 18 and 24 h, but not at 48 h. By contrast, SAMC-induced apoptosis was not reduced in the JNK2$^{-/-}$ cells at 18, 24, or 48 h, and was actually enhanced, especially at 48 h, when compared with the WT MEF cells (Fig. 6*B*). DNA flow cytometry indicated that all three types of MEF cells displayed the same extent of arrest in G_2-M after treatment with SAMC (data not shown).

Taken together with the data in Fig. 5, these findings suggest that SAMC induces apoptosis in SW480 cells through two different pathways: one occurs early after treatment with SAMC (within 24 h) and is mediated at least in part by JNK1 signaling, and the other occurs later (at 48–72 h) and is presumably a consequence of abnormal spindle assembly and M phase arrest. It is of interest that JNK1 and JNK2 appear to play different roles in this process (see Discussion).

Activation of ERK1/2 and p38 Are Not Required for SAMC-Induced Apoptosis. To investigate the possible roles of other MAPKs in SAMC-induced apoptosis, we measured the protein levels of ERK1/2 and p38 and the extent of their phosphorylation in SAMC-treated SW480 cells. Treatment of cells with SAMC (300 μM) caused a rapid (within 15–30 min) increase in the levels of both phospho-ERK1/2 and phospho-p38 without changing their total protein levels (Fig. 7*A*). To assess the functional significance of the activation of these two signaling kinases, we used specific inhibitors of MEK1/2 (PD) and p38 (SB; Ref. 21). MEK1/2 are upstream kinases of ERK1/2; therefore, the inhibition of MEK1/2 should result in the inhibition of the activation of ERK1/2. Cells were pretreated for 4 h with increasing concentrations (10–100 μM) of either PD or SB, and then were exposed to SAMC (300 μM) for 24 h. Pretreatment with 50 or 100 μM PD markedly inhibited SAMC-induced ERK1/2 phosphorylation, and pretreatment with 20–100 μM SB inhibited the formation of phospho-p38 (Fig. 7*B*). However, when we pretreated the cells with PD or SB at the concentrations that inhibited ERK1/2 or p38 phosphorylation, neither compound inhibited SAMC-induced apoptosis at 24 h (Fig. 7*C*) or at 48 h (data not shown). These results suggest that, in contrast to JNK1 activation (Figs. 4 and 5), ERK1/2 and p38 activation do not play critical roles in SAMC-induced apoptosis.

Role of Caspase Activation in SAMC-Induced Apoptosis. Because caspases are central components in the induction of apoptosis by various agents (22), we used fluorogenic peptide substrates to examine whether specific caspases are involved in the apoptotic process induced by SAMC. As shown in Fig. 8*A*, when SW480 cells were treated with SAMC (300 μM), caspase-3-like activity increased within 24 h and continued to rise until 70 h. However, during this time course, there was no significant increase in the activities of caspase-1, -6, -8, or -9 (Fig. 8*A*). Western blot analysis confirmed the activation of caspase-3 by SAMC and indicated that this was associated with the cleavage of poly(ADP-ribose) polymerase (PARP). SAC (300 μM) exhibited no significant effect on caspase activity using both methods (data not shown).

To further define the role of caspases in SAMC-induced apoptosis, we pretreated SW480 cells with the broad specificity caspase inhibitor VAD (23), at 50 or 100 μM for 1 h, and then exposed the cells to SAMC (300 μM) for another 24 or 48 h, and analyzed the cells for apoptosis by flow cytometry. As shown in Fig. 8*B*, VAD attenuated SAMC-induced apoptosis by about 50% at both 24 and 48 h. In the SAMC-treated cells, pretreatment with VAD reduced the percentage of sub-G_1 cells from 30 to 15% at 24 h, and from 44 to 22% at 48 h. This inhibition of apoptosis by VAD was similar at the 50- and 100-μM doses (Fig. 8*B*). These results demonstrate that both the early and late phases of SAMC-induced apoptosis in SW480 colon cancer cells are caspase dependent, although it is not apparent why the VAD compound did not produce 100% inhibition of apoptosis. As expected, this compound did not inhibit SAMC-induced arrest of the cell cycle in G_2-M (data not shown).

DISCUSSION

Epidemiological studies suggest that the consumption of garlic or its derivatives may have preventive effects for several types of cancer including stomach, colorectal, and prostate cancers (1, 24). Garlic and its organic sulfur components have also been shown to exert anticancer activities in both cell culture and animal carcinogenesis models of a variety of cancers (1). However, the specific component(s) of garlic that is responsible for its anticancer properties and the underlying cellular and molecular mechanisms is not known with certainty. We previously reported that SAMC, a major water-soluble compound derived from "aged garlic extract" (25), inhibits growth, arrests cells in M phase, and induces apoptosis in two human colon cancer cell lines (2). We have seen similar effects in human esophageal cancer cell lines.[4] Similar effects of SAMC on apoptosis induction and G_2-M cell cycle arrest have also been reported in erythroleukemia cell lines (26). In the present study, we examined the molecular basis of these effects. Our results indicate that the growth inhibition, M phase arrest, and induction of apoptosis produced by SAMC are associated with depolymerization of cellular MTs as a consequence of the direct interaction of this compound with tubulin. Our results provide the first evidence that a constituent of garlic suppresses MT dynamics and, thus, interferes with mitotic spindle formation. These effects resemble

[4] D. Xiao and I. B. Weinstein, unpublished data.

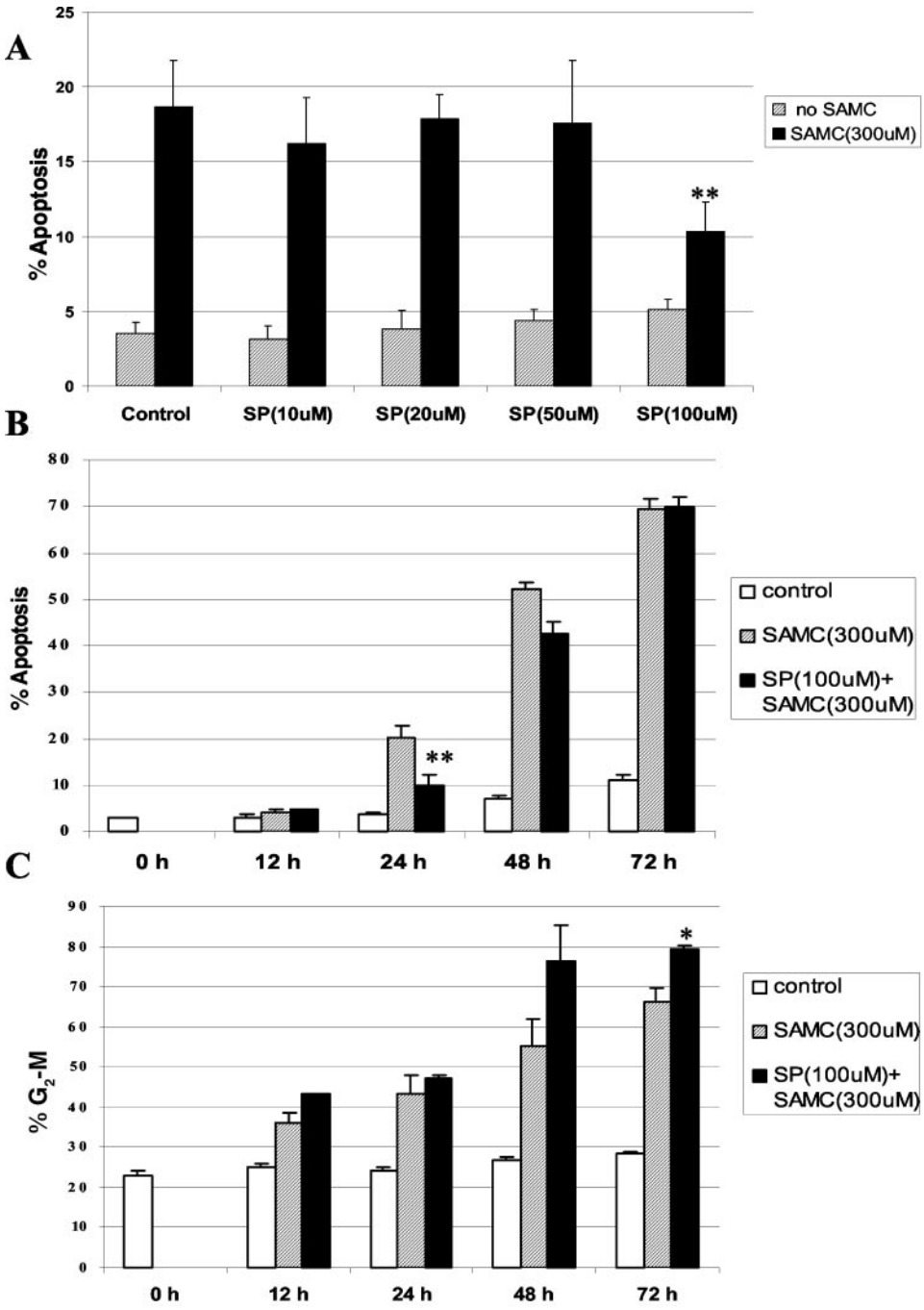

Fig. 5. Effects of SP on SAMC-induced apoptosis and G_2-M cell cycle arrest. *A*, SW480 cells were pretreated with the indicated concentrations of SP for 4 h; then the medium was removed, and the cells were treated with SAMC (300 μM) for 24 h. The cells were then harvested, stained with PI, and analyzed by flow cytometry. The percentage of apoptosis was determined as the sub-G_1 population. *B–C*, cells were pretreated with SP (100 μM) for 4 h; then the medium was removed, and the cells were exposed to SAMC (300 μM) for the indicated times. The percentage of apoptosis was then determined (*B*), and the percentage of G_2-M phase cells within the nonapoptotic population was determined by flow cytometry (*C*). Data shown are the means ± SD from three independent experiments; *, $P < 0.05$, **, $P < 0.01$, comparing the SP+SAMC-treated group with SAMC-alone-treated group.

those of the cancer chemotherapy agent Colcemid, nocodazole, and *Vinca* alkaloids. The garlic-derived compound SAMC represents a new chemical class of MT-disrupting agents, suggesting that this compound and/or derivatives might provide a novel approach to cancer chemoprevention and/or cancer therapy.

MIAs can be subdivided into classes based on their binding sites or domains on tubulin: the colchicine-binding site, the *Vinca* alkaloid-binding site, the paclitaxel-binding site, tubulin sulfhydryl groups, and uncharacterized binding sites (17). Our results indicate that SAMC interacts directly with tubulin and that MAPs may assist in this interaction (Fig. 3). Furthermore, the sulfhydryl reactive agent β-ME inhibited the ability of SAMC to cause MT depolymerization in *in vitro* turbidity assays (Fig. 3*D*), suggesting that one or more sulfhydryl (−SH) groups in tubulin form a covalent bond with SAMC. It is known that the thiol groups on cysteine residues in tubulin are highly reactive (17). There are 12 cysteine residues in α-tubulin and 8 in β-tubulin. These cysteine residues are sensitive reporters for determining the conformation of tubulin, and thiol-disulfide exchanges between them may be a key regulator of ligand interactions and MT assembly (27). Although not fully understood, oxidation or covalent interactions of certain key thiol groups (*i.e.*, Cys_{239} or Cys_{354}) can cause structural modifications of tubulin, inhibit MT assembly, and also interfere with the formation of the mitotic spindle (17, 28–30). Additional studies are required to demonstrate the direct formation of disulfide bonds between SAMC and one or more specific cysteine residues in tubulin.

In addition to these *in vitro* and *in vivo* effects on MT depolymerization, our study revealed other cellular effects of SAMC. SAMC induced centrosome fragmentation within 10 min after exposure of

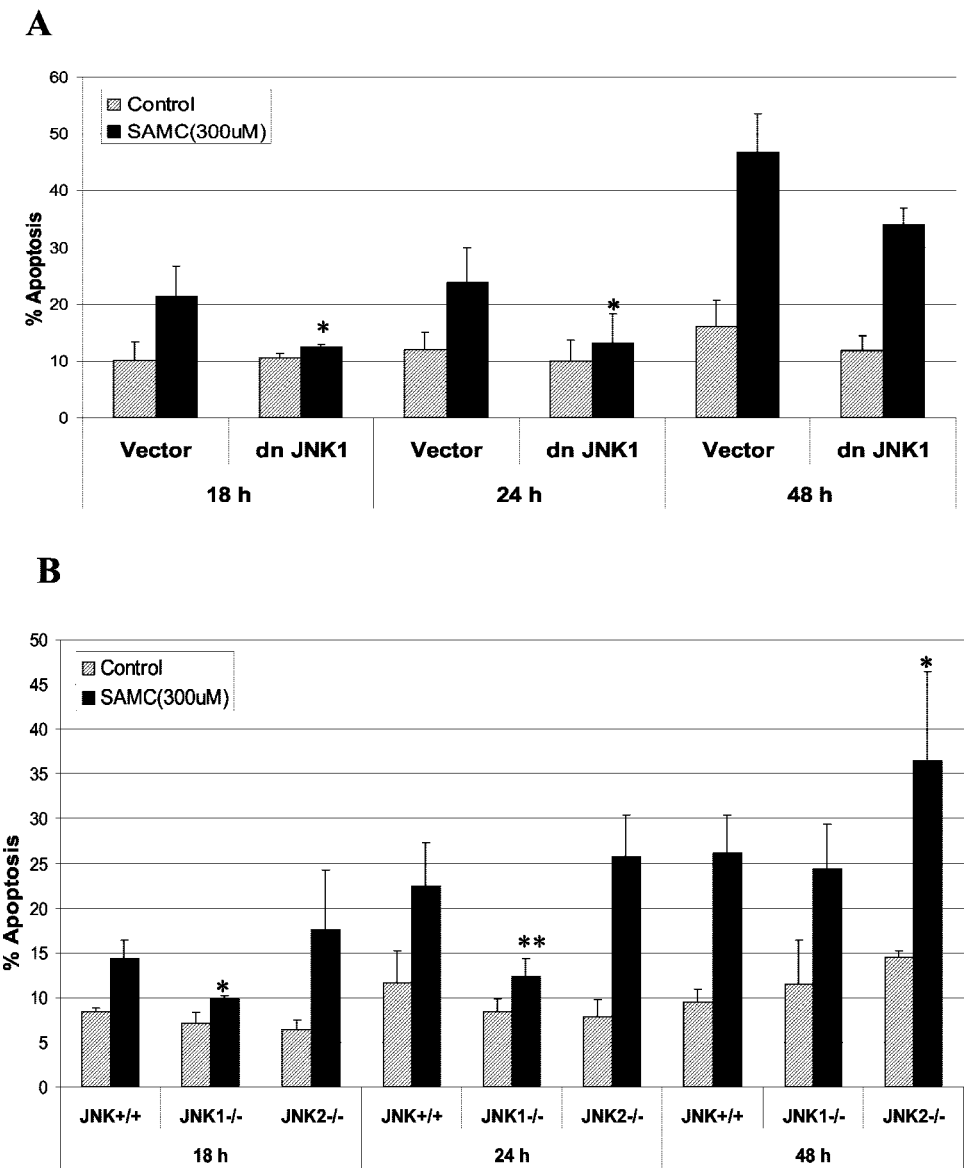

Fig. 6. *A*, effects of dn-JNK1 on SAMC-induced apoptosis. SW480 cells were cotransfected with pEGFPF and dn-JNK1 or a control vector for 24 h. They were then treated with 300 μM SAMC for the indicated times, stained with Annexin V-PE and 7-AAD, and analyzed by flow cytometry for the extent of apoptosis in the transfected cells (see "Materials and Methods"). Data shown are the means ± SD from three independent experiments; *, $P < 0.05$, comparing the dn-JNK1-transfected group with the corresponding vector control group, after treatment with SAMC. *B*, effects of SAMC on the induction of apoptosis in WT, JNK1$^{-/-}$, and JNK2$^{-/-}$ MEF cells. The three types of cells were treated with 300 μM SAMC for the indicated times. The cells were then harvested, stained with Annexin V-PE and 7-AAD, and analyzed by flow cytometry for the extent of apoptosis. Data shown are the means ± SD from three independent experiments; *, $P < 0.05$, and **, $P < 0.01$, comparing the indicated group to JNK$^{+/+}$ cells, after treatment with SAMC.

cells to this compound (Fig. 2*B*). The centrosome serves as the organization center for MTs. This fragmentation may account for the formation of multipolar spindles during mitosis in SAMC-treated cells (Fig. 1*H*). A recent report (31) indicates that monopolar spindles are induced by both MT-stabilizing and -depolymerizing agents, but that multipolar spindles are induced only by MT-stabilizing drugs (such as Taxol, epothilone B, and discodermolide), but not by MT-depolymerizing agents (such as colchicine, nocodazole, and vinblastine). Chen and Horwitz (31) suggested that the aberrant mitosis in cells with multipolar spindles may explain the higher sensitivity of cells to MT-stabilizing agents. However, our study indicates that even though SAMC is a MT-depolymerizing agent, it induced multipolar spindles, perhaps because of the unique mechanism by which it disrupts MT structure. It is well known that a close relation exists between the Golgi elements and MTs (14). We found that SAMC induced the break-up of Golgi stacks and caused their dispersal within the cytoplasm of interphase cells, an effect similar to that produced by nocodazole (14). Because an important function of the Golgi complex is the processing, sorting, and transport of membrane and luminal proteins after their synthesis, the disruption of the Golgi apparatus by SAMC may contribute to the cytotoxicity of this compound.

Our findings may also be relevant to the antitumor effects of other garlic-derived compounds. Allicin (diallyl thiosulfinate), the major ingredient of crushed garlic, has been shown to inhibit the proliferation of human breast, endometrial, and colon cancer cells (32). However, allicin is rapidly metabolized, both *in vitro* and *in vivo*, and could not be detected in human blood or urine even after a large oral dose (33). When allicin was incubated with cysteine at a physiological temperature and pH, under conditions mimicking those in the intestinal tract, it was found that allicin reacted with cysteine in less than one min and yielded two moles of SAMC per mol of allicin (34). Other garlic-derived compounds, including diallyl trisulfide, diallyl disulfide, and ajoene, were also transformed to SAMC in this *in vitro* model system (34). Furthermore, allicin can also react rapidly with glutathione- or thiol-containing proteins to produce SAMC (35, 36). These studies suggest that after the consumption of garlic, SAMC can be a major metabolic product in the intestinal tract and could, therefore, reach a high local concentration in the intestinal mucosa, thus enhancing its effects on colon cancer prevention. A recent study found that an aqueous garlic extract inhibited cell growth and markedly arrested the cell cycle at G_2-M in HT-29 human colon cancer cells. Thus, 89% of the treated cells were in G_2-M *versus* 12% in the control

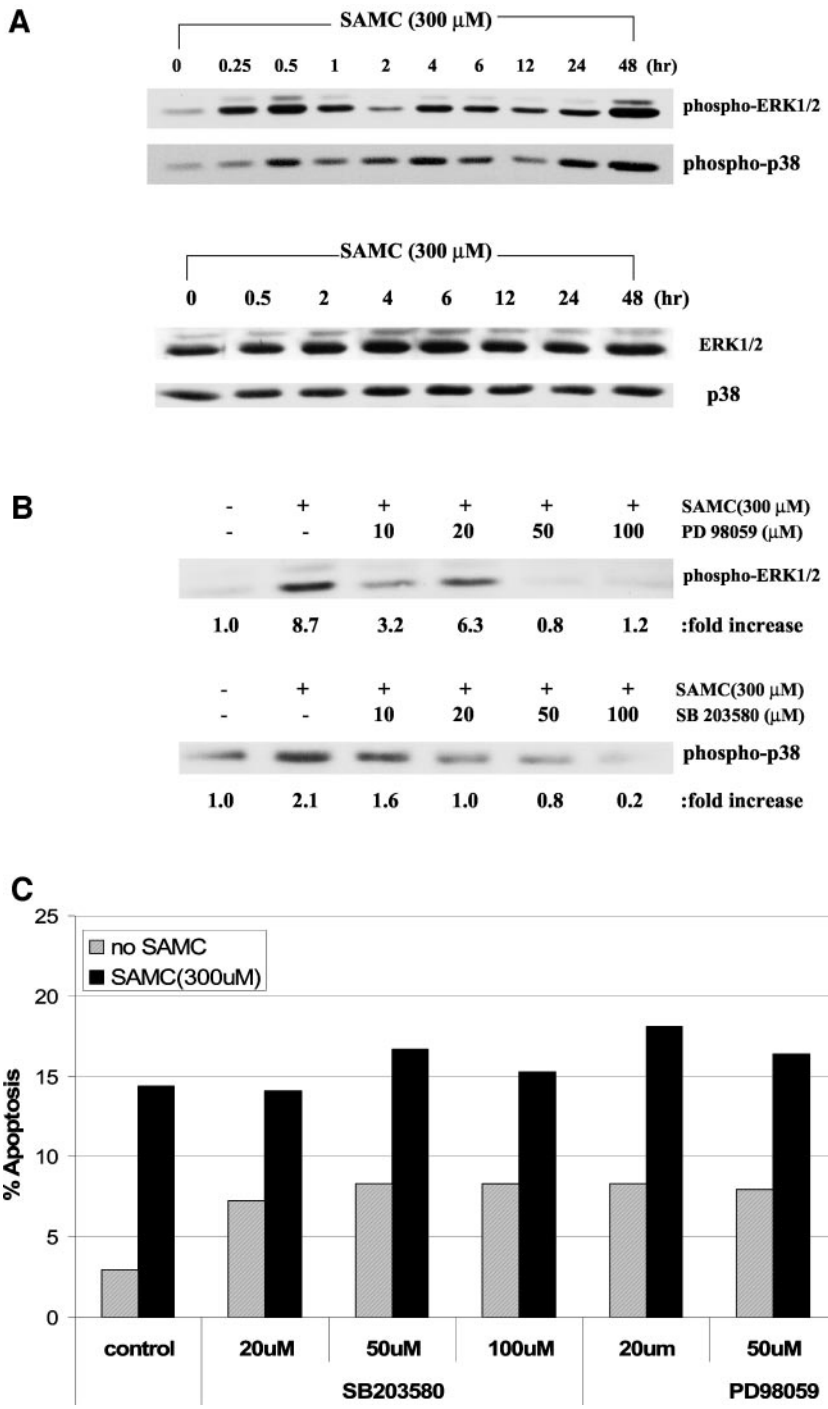

Fig. 7. Role of ERK1/2 and p38 in SAMC-induced apoptosis. *A*, SW480 cells were treated with 300 μM SAMC for the indicated times. Cell extracts were then prepared and analyzed by Western blotting using specific antibodies to ERK1/2, phospho-ERK1/2, p38, and phospho-p38. *B*, cells were pretreated with increasing concentrations (10–100 μM) of the ERK inhibitor PD or the p38 inhibitor SB for 4 h; then the medium was removed, and the cells were treated with SAMC (300 μM) for another 24 h. Cell extracts were then analyzed by Western blotting with the respective antibodies. "Fold increase" in *B* is relative to the untreated control cells. *C*, cells were pretreated with increasing concentrations (20–100 μM) of PD or SB for 4 h, then the medium was removed, and the cells were treated with SAMC (300 μM) for another 24 h. Cells were then harvested, stained with PI, and analyzed by flow cytometry. The percentage of apoptosis was determined as the sub-G_1 population. These studies were repeated and yielded similar results.

cells (37). Allicin was also found to arrest MCF-7 human breast cancer cells in G_2-M (32). Thus, it seems likely that the cellular and molecular effects of SAMC that we observed in the present study are relevant to the antitumor effects of garlic and other garlic derivatives. At the same time, our findings do not exclude the possibility that garlic and specific garlic derivatives exert antitumor effects through additional mechanisms, for example, effects on drug metabolizing enzymes (1, 38), alteration of protein phosphorylation status (39), and so forth.

In contrast to the effects of SAMC, our studies with SAC indicated that this compound does not have any detectable effects on growth, cell cycle progression, or MT polymerization in intact SW480 or NIH3T3 cells, at concentrations of 150–300 μM. These negative findings are consistent with previous reports indicating that similar concentrations of SAC failed to show growth-inhibitory effects in human colon, lung, skin, and prostate cancer cell lines (25, 40). Previous studies showed that SAC did have antiproliferative effects on neuroblastoma (41) and melanoma (42) cells, but in these studies the doses were extremely high, *i.e.*, in the range of 1–10 mM. A pharmacokinetic study (43) of SAC in rats, mice, and dogs indicated that after oral administration SAC was rapidly and efficiently absorbed in the gastrointestinal tract. In rats, the bioavailability was 98%. The maximum plasma concentration appeared within 0.5–1 h, and was 50, 112, and 227 μM after oral administration of 12.5, 25, or 50 mg/kg SAC, respectively. Unfortunately, no pharmacokinetic data are available for SAMC. It is, however, encouraging that the plasma

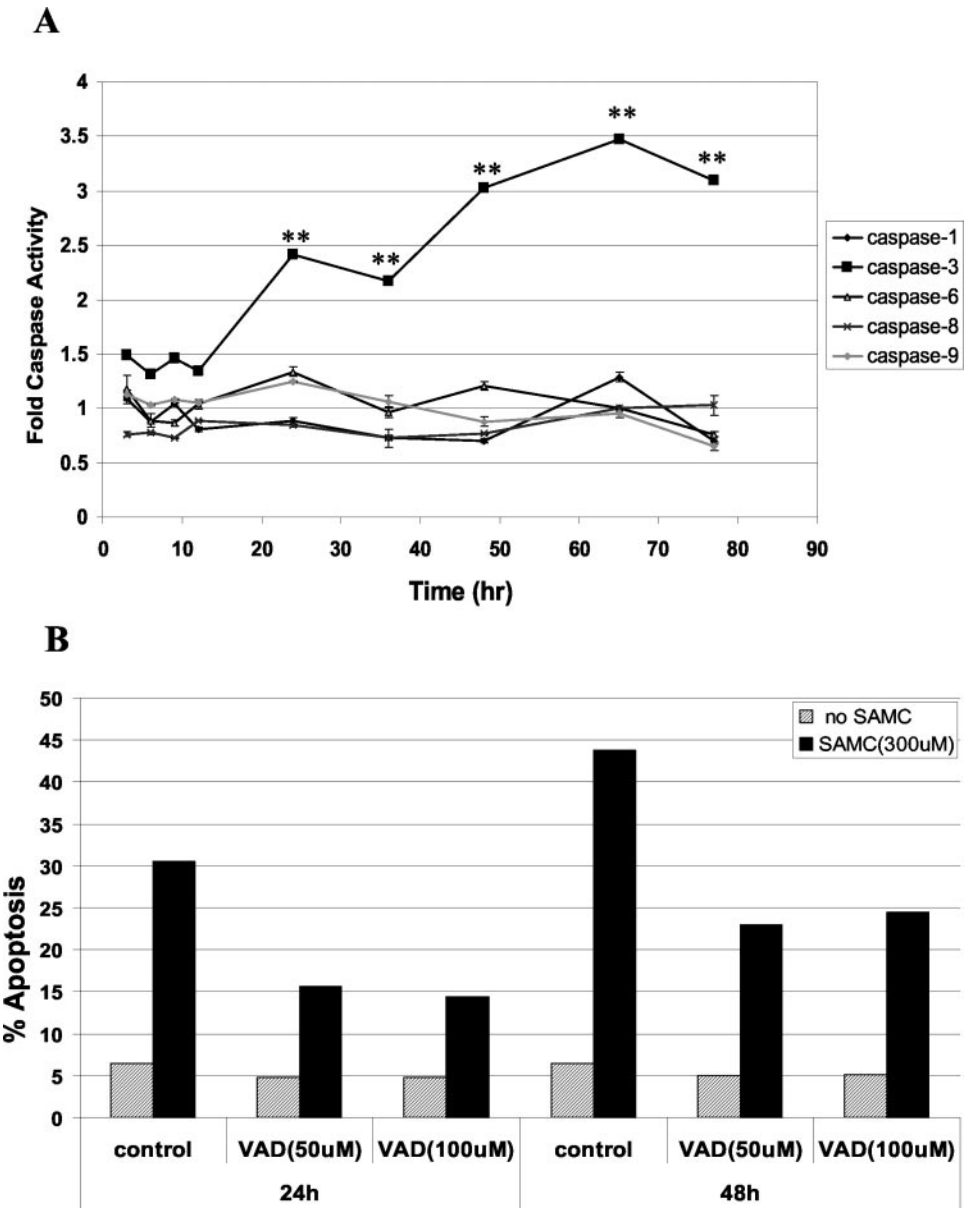

Fig. 8. *A*, Effects of SAMC and SAC on the induction of caspase activity. SW480 cells were treated with 300 μM SAMC or SAC for the indicated times. Cell extracts were then prepared and incubated at 37°C for 3 h with specific fluorogenic peptide substrate of caspase-1, -3, -6, -8, or -9, respectively. The release of fluorescence was then measured, and the corresponding caspase activity was calculated, as described in "Materials and Methods." The results are presented as the fold-increase relative to the untreated control. Data shown are the means ± SD from triplicate experiments; **, $P < 0.01$, comparing the SAMC-treated cells with the untreated control cells. *B*, effects of the general caspase inhibitor VAD on SAMC-induced apoptosis. SW480 cells were pretreated with 50 or 100 μM VAD for 1 h, then 300 μM SAMC was added to the medium, and the cells were incubated for an additional 24 or 48 h. Cells were harvested, stained with PI, and analyzed by flow cytometry. The percentage of apoptosis was determined as the sub-G_1 population. These studies were repeated and yielded similar results.

levels of SAC in the above-cited study (43) were in the range of the SAMC concentrations that we used in our cell culture studies, *i.e.*, 150–300 μM. Two *in vivo* studies showed that oral administration of SAMC (200 mg/kg) decreased acetaminophen-induced liver injury in mice, thus indicating the bioavailability of orally administrated SAMC (44, 45). It is curious that, although in our studies, SAC did not have any observable toxicity to intact cells, like SAMC, it did interfere with tubulin polymerization in *in vitro* turbidity assays (Fig. 3), presumably because it can also interact with sulfhydryl groups in purified tubulin. Presumably the lack of a cytotoxic effect of SAC in intact cells reflects the limited uptake and/or rapid metabolism of this compound by cells, but the precise mechanism remains to be determined.

Our studies of the signal transduction pathways involved in SAMC-induced apoptosis demonstrate that treatment of cells with SAMC leads to rapid, marked, and persistent activation of the JNK1 pathway (Fig. 4*A*). Presumably this contributes to the apoptotic effect of SAMC, because activation of JNK1 is known to play a role in the induction of apoptosis by other cytotoxic agents (12). Indeed, our studies with the JNK inhibitor SP, a dn-JNK1, and with $JNK1^{-/-}$ cells provide evidence that this pathway plays an important role in the early phase of apoptosis induced by SAMC, and that this effect is independent of the G_2-M cell cycle arrest induced by this compound (Figs. 5 and 6). A hypothetical scheme based on our results is shown in Fig. 9. SAMC interacts directly with tubulin and induces MT depolymerization, shortly after it enters the cells, *i.e.*, within 10 min. This leads, through unknown mechanisms, to rapid activation of the JNK1 pathway within 15 min; this, in turn, leads to activation of caspase-3, PARP cleavage, and other events that mediate an early phase of apoptosis, occurring during the first 24 h, which we designate "Phase 1." During this period, SAMC-induced MT depolymerization also interferes with assembly of the mitotic spindle, thus arresting cells in mitosis, within the first 12–24 h. Presumably, this arrest triggers spindle checkpoint and other responses, which contribute to a late phase of apoptosis, termed "Phase 2," which occurs at about 24–48 h after treatment with SAMC. We found that SAMC also causes activation of the ERK1/2 and p38 kinases (Fig. 7*A*), but the functional significance of these effects with respect to cytotoxicity are not known.

Activation of JNK1 and caspase-3 has been found in a variety of human cell cultures after exposure to both the MT-stabilizing agents (such as paclitaxel) and the MT-depolymerizing agents (such as

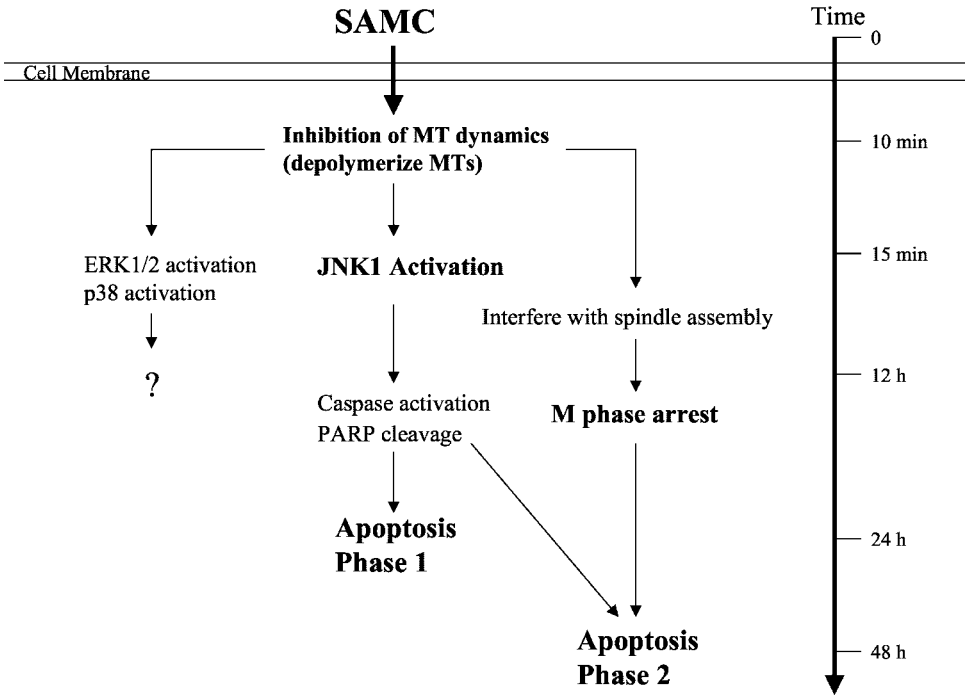

Fig. 9. Hypothetical scheme of the apoptotic signal transduction pathway activated by the MT-depolymerization agent, SAMC.

vinblastine, nocodazole, and colchicine; Refs. 12 and 46). There is also evidence that the apoptosis induced by paclitaxel is mediated through both JNK-dependent and JNK-independent pathways. Thus, when ovary cancer BR cells were treated with paclitaxel, the inhibition of the JNK1 pathway did not interfere with the mitotic arrest caused by this drug, yet it inhibited apoptotic changes induced at 16 h, but did not inhibit apoptotic events induced at 48 h after treatment with paclitaxel (47). These findings are similar to those we obtained with SAMC and are consistent with the above-discussed hypothetical model, displayed in Fig. 9. Although similar studies have not been previously reported for other MT-depolymerizing agents, it seems likely that this model may apply to diverse MIAs.

Our studies with JNK1$^{-/-}$ and JNK2$^{-/-}$ cells demonstrated that a lack of JNK1 activity inhibits SAMC-induced apoptosis, whereas a lack of JNK2 activity actually enhances SAMC-induced apoptosis (Fig. 6*B*), indicating different roles for JNK1 and JNK2 in these cellular events. Our findings are consistent with previous evidence that JNK1 is specifically involved in mediating the apoptotic response in a variety of human cancer cells treated with UV radiation or MIAs (12, 48), whereas JNK2 plays a more specific role in cell survival (49). In a DMBA/TPA two-stage skin tumor model, JNK1$^{-/-}$ mice were more susceptible to TPA-induced skin tumor formation and growth than were WT mice (50), whereas skin tumorigenesis was suppressed in JNK2$^{-/-}$ mice (51). These findings suggest that JNK1 normally suppresses DMBA/TPA-induced skin tumor development, whereas JNK2 enhances it. A cDNA microarray analysis revealed different patterns of gene expression in JNK1$^{-/-}$, JNK2$^{-/-}$, and WT MEFs after TPA treatment (5). In JNK1$^{-/-}$ cells, TPA upregulated 16 genes, including the genes encoding well-known antiapoptotic proteins, such as the *A20* zinc finger protein, *GST5-5*, and the *c-akt* oncoprotein. In TPA-treated JNK2$^{-/-}$ cells, most of the genes that were highly expressed were related to tumor suppression and induction of cell differentiation, apoptosis, and cell growth arrest (5). These findings appear to explain the results obtained with respect to the mouse skin tumor model (50, 51) and are also consistent with our results.

It appears that, in NIH3T3 cells, one-third of the total cellular content of MAPK is associated with the MT cytoskeleton (52). In addition, mixed linkage kinase 2 (MLK2), a MAPK kinase kinase, interacts with two KIF3 kinesin motor proteins and colocalizes with dually phosphorylated JNK1/2 in punctuate structures distributed along MTs (53). These studies indicate that several signaling molecules localize on MTs, and suggest that MTs may act as a scaffold to bring together related signaling components. This association may explain the above-described correlations between activation of MAPK activities and disruptions in MT structure caused by various drugs. Studies are in progress to examine these effects with respect to the action of SAMC. Additional studies are also required to elucidate how the arrest of cells in mitosis induced by SAMC and other MIAs leads to what we have termed the Phase 2 apoptotic response. Inactivation of the antiapoptotic protein Bcl-2 by phosphorylation has been implicated in the apoptosis induced by paclitaxel (47), but this mechanism is controversial (54). Answers to the above questions will increase our understanding of the molecular mechanisms by which MIAs exert antitumor effects and will also help in the identification and/or synthesis of novel anticancer compounds.

In summary, the present studies provide the first evidence that the garlic derivative SAMC can inhibit the growth of cancer cells by directly binding to sulfhydryl residues in tubulin and thereby disrupt MT structures in the cytoplasm of interphase cells and the spindle apparatus of mitotic cells. We have also obtained evidence that the apoptosis induced by this compound is related, at least in part, to activation of the JNK1 pathway, but additional signaling mechanisms remain to be elucidated. Our findings may encourage the development of derivatives of SAMC that are more potent and suggest that SAMC or related compounds might provide a novel approach to cancer chemoprevention and/or cancer therapy.

ACKNOWLEDGMENTS

We thank Wakunaga of America Co. for the supply of SAMC and SAC compound, Dr. Zigang Dong (University of Minnesota) for providing the JNK WT and knockout MEFs, Dr. Wei Jiang (The Salk Institute) for providing the pEGFPF plasmid, Dr. Audrey Minden (Columbia University) for providing the pCMV-DN-JNK1 plasmid, and Dr. Jeremy Luban (Columbia University) for the use of the Spectramax O.D. Reader and Gemini Fluoro/Luminometer.

REFERENCES

1. Pinto, J. T., Lapsia, S., Shah, A., Santiago, H., and Kim, G. Antiproliferative effects of garlic-derived and other allium related compounds. *In:* American Institute for Cancer Research (eds.), Nutrition and Cancer Prevention: New Insights into the Role of Phytochemicals, pp. 83–106. New York: Kluwer Academic/Plenum Publishers, 2000.
2. Shirin, H., Pinto, J. T., Kawabata, Y., Soh, J. W., Delohery, T., Moss, S. F., Murty, V., Rivlin, R. S., Holt, P. R., and Weinstein, I. B. Antiproliferative effects of *S*-allylmercaptocysteine on colon cancer cells when tested alone or in combination with sulindac sulfide. Cancer Res., *61:* 725–731, 2001.
3. Wilson, L., and Jordan, M. A. Microtubule dynamics: taking aim at a moving target. Chem. Biol., *2:* 569–573, 1995.
4. Wilson, L., and Jordan, M. A. Pharmacological probes of microtubule function. *In:* J. S. Hyams and C. W. Lloyd (eds.), Microtubules, pp. 59–83. New York: Wiley-Liss, 1994.
5. Chen, N., She, Q. B., Bode, A. M., and Dong, Z. Differential gene expression profiles of Jnk1- and Jnk2-deficient murine fibroblast cells. Cancer Res., *62:* 1300–1304, 2002.
6. Joe, A. K., Liu, H., Suzui, M., Vural, M. E., Xiao, D., and Weinstein, I. B. Resveratrol induces growth inhibition, S-phase arrest, apoptosis, and changes in biomarker expression in several human cancer cell lines. Clin. Cancer Res., *8:* 893–903, 2002.
7. Soh, J. W., Mao, Y., Kim, M. G., Pamukcu, R., Li, H., Piazza, G. A., Thompson, W. J., and Weinstein, I. B. Cyclic GMP mediates apoptosis induced by sulindac derivatives via activation of c-Jun NH_2-terminal kinase 1. Clin. Cancer Res., *6:* 4136–4141, 2000.
8. Dan, C., Nath, N., Liberto, M., and Minden, A. PAK5, a new brain-specific kinase, promotes neurite outgrowth in N1E- 115 cells. Mol. Cell. Biol., *22:* 567–577, 2002.
9. Jiang, W., and Hunter, T. Analysis of cell-cycle profiles in transfected cells using a membrane-targeted GFP. BioTechniques, *24:* 348–354, 1998.
10. Yoon, J. T., Palazzo, A. F., Xiao, D., Delohery, T. M., Warburton, P. E., Bruce, J. N., Thompson, W. J., Sperl, G., Whitehead, C., Fetter, J., Pamukcu, R., Gundersen, G. G., and Weinstein, I. B. CP248, a derivative of exisulind, causes growth inhibition, mitotic arrest, and abnormalities in microtubule polymerization in glioma cells. Mol. Cancer Ther., *1:* 393–404, 2002.
11. Kilmartin, J. V., Wright, B., and Milstein, C. Rat monoclonal antitubulin antibodies derived by using a new nonsecreting rat cell line. J. Cell Biol., *93:* 576–582, 1982.
12. Wang, T. H., Wang, H. S., Ichijo, H., Giannakakou, P., Foster, J. S., Fojo, T., and Wimalasena, J. Microtubule-interfering agents activate c-Jun N-terminal kinase/stress-activated protein kinase through both Ras and apoptosis signal-regulating kinase pathways. J. Biol. Chem., *273:* 4928–4936, 1998.
13. Logan, T. J., Jordan, K. L., and Hall, D. Altered shape and cell cycle characteristics of fibroblasts expressing the E2F1 transcription factor. Mol. Biol. Cell, *5:* 667–678, 1994.
14. Thyberg, J., and Moskalewski, S. Role of microtubules in the organization of the Golgi complex. Exp. Cell Res., *246:* 263–279, 1999.
15. Keates, R. A., and Mason, G. B. Inhibition of microtubule polymerization by the tubulin-colchicine complex: inhibition of spontaneous assembly. Can. J. Biochem., *59:* 361–370, 1981.
16. Schiff, P. B., and Horwitz, S. B. Taxol assembles tubulin in the absence of exogenous guanosine 5′-triphosphate or microtubule-associated proteins. Biochemistry, *20:* 3247–3252, 1981.
17. Jordan, A., Hadfield, J. A., Lawrence, N. J., and McGown, A. T. Tubulin as a target for anticancer drugs: agents which interact with the mitotic spindle. Med. Res. Rev., *18:* 259–296, 1998.
18. Jiang, J. D., Denner, L., Ling, Y. H., Li, J. N., Davis, A., Wang, Y., Li, Y., Roboz, J., Wang, L. G., Perez-Soler, R., Marcelli, M., Bekesi, G., and Holland, J. F. Double blockade of cell cycle at G1-S transition and M phase by 3-iodoacetamido benzoyl ethyl ester, a new type of tubulin ligand. Cancer Res., *62:* 6080–6088, 2002.
19. Bennett, B. L., Sasaki, D. T., Murray, B. W. O'Leary, E. C., Sakata, S. T., Xu, W., Leisten, J. C., Motiwala, A., Pierce, S., Satoh, Y., Bhagwat, S. S., Manning, A. M., and Anderson, D. W. SP600125, an anthrapyrazolone inhibitor of Jun N-terminal kinase. Proc. Natl. Acad. Sci. USA, *98:* 13681–13686, 2001.
20. Han, Z., Boyle, D. L., Chang, L., Bennett, B., Karin, M., Yang, L., Manning, A. M., and Firestein, G. S. c-Jun N-terminal kinase is required for metalloproteinase expression and joint destruction in inflammatory arthritis. J. Clin. Investig., *108:* 73–81, 2001.
21. Tseng, C. J., Wang, Y. J., Liang, Y. C., Jeng, J. H., Lee, W. S., Lin, J. K., Chen, C., Liu, I. C., and Ho, Y. S. Microtubule damaging agents induce apoptosis in HL 60 cells and G_2/M cell cycle arrest in HT 29 cells. Toxicology, *175:* 123–142, 2002.
22. Thornberry, N. A., and Lazebnik, Y. Caspases: enemies within. Science (Wash. DC), *281:* 1312–1316, 1998.
23. Mandlekar, S., Yu, R., Tan, T. H., and Kong, A. N. Activation of caspase-3 and c-Jun NH_2-terminal kinase-1 signaling pathways in tamoxifen-induced apoptosis of human breast cancer cells. Cancer Res., *60:* 5995–6000, 2000.
24. Hsing, A. W., Chokkalingam, A. P., Gao, Y. T., Madigan, M. P., Deng, J., Gridley, G., and Fraumeni, J. F., Jr. Allium vegetables and risk of prostate cancer: a population-based study. J. Natl. Cancer Inst. (Bethesda), *94:* 1648–1651, 2002.
25. Pinto, J. T., Qiao, C., Xing, J., Rivlin, R. S., Protomastro, M. L., Weissler, M. L., Tao, Y., Thaler, H., and Heston, W. D. Effects of garlic thioallyl derivatives on growth, glutathione concentration, and polyamine formation of human prostate carcinoma cells in culture. Am. J. Clin. Nutr., *66:* 398–405, 1997.
26. Sigounas, G., Hooker, J. L., Li, W., Anagnostou, A., and Steiner, M. S-allylmercaptocysteine, a stable thioallyl compound, induces apoptosis in erythroleukemia cell lines. Nutr. Cancer, *28:* 153–159, 1997.
27. Chaudhuri, A. R., Khan, I. A., and Luduena, R. F. Detection of disulfide bonds in bovine brain tubulin and their role in protein folding and microtubule assembly *in vitro*: a novel disulfide detection approach. Biochemistry, *40:* 8834–8841, 2001.
28. Luduena, R. F., and Roach, M. C. Tubulin sulfhydryl groups as probes and targets for antimitotic and antimicrotubule agents. Pharmacol. Ther., *49:* 133–152, 1991.
29. Legault, J., Gaulin, J. F., Mounetou, E., Bolduc, S., Lacroix, J., Poyet, P., and Gaudreault, R. C. Microtubule disruption induced in vivo by alkylation of β-tubulin by 1-aryl-3-(2-chloroethyl)ureas, a novel class of soft alkylating agents. Cancer Res., *60:* 985–992, 2000.
30. Shan, B., Medina, J. C., Santha, E., Frankmoelle, W. P., Chou, T. C., Learned, R. M., Narbut, M. R., Stott, D., Wu, P., Jaen, J. C., Rosen, T., Timmermans, P. B., and Beckmann, H. Selective, covalent modification of beta-tubulin residue Cys-239 by T138067, an antitumor agent with *in vivo* efficacy against multidrug-resistant tumors. Proc. Natl. Acad. Sci. USA, *96:* 5686–5691, 1999.
31. Chen, J. G., and Horwitz, S. B. Differential mitotic responses to microtubule-stabilizing and -destabilizing drugs. Cancer Res., *62:* 1935–1938, 2002.
32. Hirsch, K., Danilenko, M., Giat, J., Miron, T., Rabinkov, A., Wilchek, M., Mirelman, D., Levy, J., and Sharoni, Y. Effect of purified allicin, the major ingredient of freshly crushed garlic, on cancer cell proliferation. Nutr. Cancer, *38:* 245–254, 2000.
33. Lawson, L. D., Ransom, D. K., and Hughes, B. G. Inhibition of whole blood platelet-aggregation by compounds in garlic clove extracts and commercial garlic products. Thromb. Res., *65:* 141–156, 1992.
34. Lawson, L. D., and Wang, Z. J. Pre-hepatic fate of the organosulfur compounds derived from garlic (*Allium sativum*). Planta Med., *59* (Suppl.)*:* A688–A689, 1993.
35. Rabinkov, A., Miron, T., Konstantinovski, L., Wilchek, M., Mirelman, D., and Weiner, L. The mode of action of allicin: trapping of radicals and interaction with thiol containing proteins. Biochim. Biophys. Acta, *1379:* 233–244, 1998.
36. Rabinkov, A., Miron, T., Mirelman, D., Wilchek, M., Glozman, S., Yavin, E., and Weiner, L. *S*-Allylmercaptoglutathione: the reaction product of allicin with glutathione possesses SH-modifying and antioxidant properties. Biochim. Biophys. Acta, *1499:* 144–153, 2000.
37. Frantz, D. J., Hughes, B. G., Nelson, D. R., Murray, B. K., and Christensen, M. J. Cell cycle arrest and differential gene expression in HT-29 cells exposed to an aqueous garlic extract. Nutr. Cancer, *38:* 255–264, 2000.
38. Munday, R., and Munday, C. M. Relative activities of organosulfur compounds derived from onions and garlic in increasing tissue activities of quinone reductase and glutathione transferase in rat tissues. Nutr. Cancer, *40:* 205–210, 2001.
39. Lee, E. S., Steiner, M., and Lin, R. Thioallyl compounds: potent inhibitors of cell proliferation. Biochim. Biophys. Acta, *1221:* 73–77, 1994.
40. Sundaram, S. G., and Milner, J. A. Diallyl disulfide inhibits the proliferation of human tumor cells in culture. Biochim. Biophys. Acta, *1315:* 15–20, 1996.
41. Welch, C., Wuarin, L., and Sidell, N. Antiproliferative effect of the garlic compound *S*-allyl cysteine on human neuroblastoma cells *in vitro*. Cancer Lett., *63:* 211–219, 1992.
42. Takeyama, H., Hoon, D. S., Saxton, R. E., Morton, D. L., and Irie, R. F. Growth inhibition and modulation of cell markers of melanoma by *S*-allyl cysteine. Oncology, *50:* 63–69, 1993.
43. Nagae, S., Ushijima, M., Hatono, S., Imai, J., Kasuga, S., Matsuura, H., Itakura, Y., and Higashi, Y. Pharmacokinetics of the garlic compound *S*-allylcysteine. Planta Med., *60:* 214–217, 1994.
44. Sumioka, I., Matsura, T., Kasuga, S., Itakura, Y., and Yamada, K. Mechanisms of protection by *S*-allylmercaptocysteine against acetaminophen-induced liver injury in mice. Jpn. J. Pharmacol., *78:* 199–207, 1998.
45. Sumioka, I., Matsura, T., and Yamada, K. Therapeutic effect of *S*-allylmercaptocysteine on acetaminophen-induced liver injury in mice. Eur. J. Pharmacol., *433(2–3):* 177–185, 2001.
46. Gorman, A. M., Bonfoco, E., Zhivotovsky, B., Orrenius, S., and Ceccatelli, S. Cytochrome c release and caspase-3 activation during colchicine-induced apoptosis of cerebellar granule cells. Eur. J. Neurosci., *11:* 1067–1072, 1999.
47. Wang, T. H., Popp, D. M., Wang, H. S., Saitoh, M., Mural, J. G., Henley, D. C., Ichijo, H., and Wimalasena, J. Microtubule dysfunction induced by paclitaxel initiates apoptosis through both c-Jun N-terminal kinase (JNK)-dependent and -independent pathways in ovarian cancer cells. J. Biol. Chem., *274:* 8208–8216, 1999.
48. Butterfield, L., Storey, B., Maas, L., and Heasley, L. E. c-Jun NH_2-terminal kinase regulation of the apoptotic response of small cell lung cancer cells to ultraviolet radiation. J. Biol. Chem., *272:* 10110–10116, 1997.
49. Wojtaszek, P. A., Heasley, L. E., Siriwardana, G., and Berl, T. Dominant-negative c-Jun NH2-terminal kinase 2 sensitizes renal inner medullary collecting duct cells to hypertonicity-induced lethality independent of organic osmolyte transport. J. Biol. Chem., *273:* 800–804, 1998.
50. She, Q. B., Chen, N., Bode, A. M., Flavell, R. A., and Dong, Z. Deficiency of c-Jun-NH_2-terminal kinase-1 in mice enhances skin tumor development by 12-*O*-tetradecanoylphorbol-13-acetate. Cancer Res., *62:* 1343–1348, 2002.
51. Chen, N., Nomura, M., She, Q. B., Ma, W. Y., Bode, A. M., Wang, L., Flavell, R. A., and Dong, Z. Suppression of skin tumorigenesis in c-Jun NH_2-terminal kinase-2-deficient mice. Cancer Res., *61:* 3908–3912, 2001.
52. Reszka, A. A., Seger, R., Diltz, C. D., Krebs, E. G., and Fischer, E. H. Association of mitogen-activated protein kinase with the microtubule cytoskeleton. Proc. Natl. Acad. Sci. USA, *92:* 8881–8885, 1995.
53. Nagata, K., Puls, A., Futter, C., Aspenstrom, P., Schaefer, E., Nakata, T., Hirokawa, N., and Hall, A. The MAP kinase kinase kinase MLK2 co-localizes with activated JNK along microtubules and associates with kinesin superfamily motor KIF3. EMBO J., *17:* 149–158, 1998.
54. Ling, Y. H., Tornos, C., and Perez-Soler, R. Phosphorylation of Bcl-2 is a marker of M phase events and not a determinant of apoptosis. J. Biol. Chem., *273:* 18984–18991, 1998.

Induction of Apoptosis by the Garlic-Derived Compound *S*-Allylmercaptocysteine (SAMC) Is Associated with Microtubule Depolymerization and c-Jun NH $_2$-Terminal Kinase 1 Activation

Danhua Xiao, John T. Pinto, Jae-Won Soh, et al.

Cancer Res 2003;63:6825-6837.